Research Article | Vol. 7, No. 10 | 1 Oct 2016 | BIOMEDICAL OPTICS EXPRESS 3951

Biomedical Optics EXPRESS

Simultaneous *in vivo* imaging of diffuse optical reflectance, optoacoustic pressure and ultrasonic scattering

PAVEL SUBOCHEV,[1,*] ANNA ORLOVA,[1] IRINA MIKHAILOVA,[1] NATALIA SHILYAGINA,[2] AND ILYA TURCHIN[1]

[1]*Institute of Applied Physics RAS, 46 Ulyanov Street, Nizhniy Novgorod, Russia*
[2]*Lobachevsky State University of Nizhny Novgorod, 19 Gagarin Avenue, Nizhniy Novgorod, Russia*
[*]*Pavel.Subochev@gmail.com*

Abstract: We present reflection-mode bioimaging system providing complementary optical, photoacsoutic and acoustic measurements by acoustic detector after each laser pulse. While the photons absorbed within the sample provide optoacoustic (OA) signals, the photons absorbed by the external electrode of a detector provide the measurable diffuse reflectance (DR) from the sample and the probing ultrasonic (US) pulse. To demonstrate the *in vivo* capabilities of the system we present the results of complementary DR/OA/US imaging of a mouse tumor, head of a newborn rat, and the back of a newborn rat with 3.5mm/50μm/35μm lateral resolution. Trimodal approach allows visualization of mechanical structures in healthy and pathological tissues along with peculiarities of blood supply. The system may be used for diagnostics of diseases accompanied by the defects of vascularization as well as for assessing the mechanisms of vascular changes when monitoring response to therapy.

©2016 Optical Society of America

OCIS codes: (170.5120) Photoacoustic imaging, (170.7180) Ultrasound diagnostics.

References and links

1. L. E. Jennings and N. J. Long, "'Two is better than one'—probes for dual-modality molecular imaging," Chem. Commun. (Camb.) **24**, 3511–3524 (2009).
2. C. J. H. Ho, N. C. Burton, S. Morscher, U. Dinish, J. Reber, V. Ntziachristos, and M. Olivo, "Advances in Optoacoustic Imaging: From Benchside to Clinic," in *Frontiers in Biophotonics for Translational Medicine* (Springer, 2016), pp. 75–109.
3. A. Taruttis and V. Ntziachristos, "Advances in real-time multispectral optoacoustic imaging and its applications," Nat. Photonics **9**(4), 219–227 (2015).
4. L. V. Wang, "Multiscale photoacoustic microscopy and computed tomography," Nat. Photonics **3**(9), 503–509 (2009).
5. P. Beard, "Biomedical photoacoustic imaging," Interface focus, rsfs20110028 (2011).
6. V. V. Tuchin and V. Tuchin, *Tissue Optics: Light Scattering Methods and Instruments for Medical Diagnosis* (SPIE press Bellingham, 2007), Vol. 13.
7. C. R. Hill, J. C. Bamber, and G. Haar, *Physical Principles of Medical Ultrasonics* (Wiley Online Library, 2004), Vol. 2.
8. H. Yang, L. Xi, S. Samuelson, H. Xie, L. Yang, and H. Jiang, "Handheld miniature probe integrating diffuse optical tomography with photoacoustic imaging through a MEMS scanning mirror," Biomed. Opt. Express **4**(3), 427–432 (2013).
9. J. J. Niederhauser, M. Jaeger, R. Lemor, P. Weber, and M. Frenz, "Combined ultrasound and optoacoustic system for real-time high-contrast vascular imaging in vivo," IEEE Trans. Med. Imaging **24**(4), 436–440 (2005).
10. R. Bouchard, O. Sahin, and S. Emelianov, "Ultrasound-guided photoacoustic imaging: current state and future development," IEEE Trans. Ultrason. Ferroelectr. Freq. Control **61**(3), 450–466 (2014).
11. P. Subochev, A. Katichev, A. Morozov, A. Orlova, V. Kamensky, and I. Turchin, "Simultaneous photoacoustic and optically mediated ultrasound microscopy: phantom study," Opt. Lett. **37**(22), 4606–4608 (2012).
12. P. Subochev, A. Orlova, M. Shirmanova, A. Postnikova, and I. Turchin, "Simultaneous photoacoustic and optically mediated ultrasound microscopy: an in vivo study," Biomed. Opt. Express **6**(2), 631–638 (2015).
13. P. Subochev, I. Fiks, M. Frenz, and Turchin, "Simultaneous triple-modality imaging of diffuse reflectance, optoacoustic pressure and ultrasonic scattering using an acoustic-resolution photoacoustic microscope: feasibility study," Laser Phys. Lett. **13**(2), 025605 (2016).
14. P. Subochev, "Cost-effective imaging of optoacoustic pressure, ultrasonic scattering, and optical diffuse reflectance with improved resolution and speed," Opt. Lett. **41**(5), 1006–1009 (2016).

#268181 http://dx.doi.org/10.1364/BOE.7.003951
Journal © 2016 Received 10 Jun 2016; revised 3 Sep 2016; accepted 6 Sep 2016; published 12 Sep 2016

Biomedical Optics EXPRESS

15. D. Bergström, J. Powell, and A. Kaplan, "A ray-tracing analysis of the absorption of light by smooth and rough metal surfaces," J. Appl. Phys. **101**(11), 113504 (2007).
16. M.-L. Li, H. E. Zhang, K. Maslov, G. Stoica, and L. V. Wang, "Improved in vivo photoacoustic microscopy based on a virtual-detector concept," Opt. Lett. **31**(4), 474–476 (2006).
17. M. Jaeger, S. Schüpbach, A. Gertsch, M. Kitz, and M. Frenz, "Fourier reconstruction in optoacoustic imaging using truncated regularized inverse k-space interpolation," Inverse Probl. **23**(6), S51–S63 (2007).
18. M. Omar, M. Schwarz, D. Soliman, P. Symvoulidis, and V. Ntziachristos, "Pushing the optical imaging limits of cancer with multi-frequency-band raster-scan optoacoustic mesoscopy (RSOM)," Neoplasia **17**(2), 208–214 (2015).
19. A. P. Jathoul, J. Laufer, O. Ogunlade, B. Treeby, B. Cox, E. Zhang, P. Johnson, A. R. Pizzey, B. Philip, T. Marafioti, M. F. Lythgoe, R. B. Pedley, M. A. Pule, and P. Beard, "Deep in vivo photoacoustic imaging of mammalian tissues using a tyrosinase-based genetic reporter," Nat. Photonics **22**, 10 (2015).
20. H. Estrada, J. Turner, M. Kneipp, and D. Razansky, "Real-time optoacoustic brain microscopy with hybrid optical and acoustic resolution," Laser Phys. Lett. **11**(4), 045601 (2014).
21. J. Yao, L. Wang, J.-M. Yang, K. I. Maslov, T. T. Wong, L. Li, C.-H. Huang, J. Zou, and L. V. Wang, "High-speed label-free functional photoacoustic microscopy of mouse brain in action," Nat. Methods **12**(5), 407–410 (2015).
22. A. Q. Bauer, R. E. Nothdurft, T. N. Erpelding, L. V. Wang, and J. P. Culver, "Quantitative photoacoustic imaging: correcting for heterogeneous light fluence distributions using diffuse optical tomography," J. Biomed. Opt. **16**, 096016 (2011).
23. A. Rosenthal, D. Razansky, and V. Ntziachristos, "Fast semi-analytical model-based acoustic inversion for quantitative optoacoustic tomography," IEEE Trans. Med. Imaging **29**(6), 1275–1285 (2010).
24. S. L. Jacques, "Coupling 3D Monte Carlo light transport in optically heterogeneous tissues to photoacoustic signal generation," Photoacoustics **2**(4), 137–142 (2014).
25. B. Cox, J. G. Laufer, S. R. Arridge, and P. C. Beard, "Quantitative spectroscopic photoacoustic imaging: a review," J. Biomed. Opt. **17**(6), 061202 (2012).

1. Introduction

Modern experimental and clinical medicine requires new diagnostic methods, that would allow to image different anatomical structures together with investigation of different physiological and pathological *in vivo* processes in real time [1].

One of the developing diagnostic tool capable of providing structural, functional and molecular information is optoacoustic (OA) imaging [2]. OA methods are based on registration of ultrasonic (US) waves due to the selective absorption of laser pulses by optical chromophores. Hybrid nature of OA methods allows to combine spectral optical contrast and scalable acoustical resolution at millimeter to centimiters diagnostic depths [3–5]. Nevertheless, to provide advanced information about *in vivo* objects, optical [6] and acoustical [7] modalities are often used together with the OA one.

An example of reflection-mode setup combining OA and diffuse reflectance (DR) measurements was reported in reference [8]. OA/DR modalities were realized in reference [8] independently, each modality utilized its own pulsed/continuous laser sourse and acoustical/optical detector. Similarities in OA and US detection allow to use single US transducer for dual-modality OA/US imaging [9]. The examples of reflection-mode combination of OA and US imaging modalities were provided in a review article [10]. To simplify dual-modality OA/US system it is also possible to replace the electrical generation of probing US pulses by laser-ultrasound one [11, 12].

In article [13] the opportunity to use an acoustic detector for complementary measurement of DR/OA/US signals after irradiation of the investigated tissue with single laser pulse was reported. Phantom study [14] announced the improved trimple-modality DR/OA/US system and demonstrated the correlations of DR images with lateral positions of scattering and absorbing structures. The present article is devoted to the first *in vivo* approbation of the same system [14]. While OA/US *in vivo* images might be interesting in terms of fourfold improvement in lateral resolution [12], DR images of *in vivo* structures might be interesting from the perspective of exploiting DR images to calibrate OA measurements and thus to obtain more quantitative results.

Biomedical Optics EXPRESS

2. Materials and methods

Figure 1 presents the principle of simultaneous DR/OA/US imaging. When the laser pulse interacts with the sample, there are two types of photons important for trimodal visualization. Photons that reach optical absorbers (Fig. 1) generate OA signal. The back-scattered photons being absorbed by a metalized surface of acoustic detector provide both the DR signal and the probing US pulse (Fig. 1). Therefore, single laser pulse allows complementary measurement of diffuse optical reflectance, optoacoustic pressure and ultrasonic scattering.

The lateral resolution of OA/US modalities 50 μm/35 μm was provided by focal spot of spherically-focused 35 MHz polyvinylidene fluoride (PVDF) detector with a 30 MHz bandwidth, F = 6.8 mm focal distance, and 0.6 numerical aperture. The lateral resolution of DR modality 3.5 mm was majorly provided by the focal spot of the light delivery system consisting of 77 optical fibers with 0.12 numerical aperture [14]. However, the spherical surface of PVDF detector can also be responsible for lateral resolution of DR modality, since the photons directing from the geometrical focus of PVDF detector are absorbed more effectively, than the photons with the different angles of incidence [15].

The scanning head (Fig. 1) was mounted on two computer-driven M-664 stages with a 25 mm travel range and 400 mm/s maximum velocity. The low-jitter input of the laser Wedge HB 532 (BrightSolutions, Italy) was triggered by the scanning stages and provided a pulse repetition rate of up to 2 kHz with a 1.4 ns pulse duration and a maximum pulse energy of 1 mJ at 532 nm. The average radiant exposure at the sample surface was 5 mJ/cm^2 complying with ANSI Z136.1 standard for laser safety.

All animal subjects used for trimodal imaging were handled in accordance with with international rules of legal and ethical use of animals. A three day old outbred rat and an eight week old balb/c-nude mouse were used in the experiments. Human breast carcinoma SKBR3 (5 × 10^6 cells) were injected subcutaneously. Tumor was imaged on the 25th day after inoculation. Before the investigation the rat was anaesthetized with an intraperitoneal injection of 50 mg/kg of Zoletil 100 and immobilized in a prone position. The mouse was anaesthetized with an intramuscular injection of Zoletil 100 (40 mg/kg) and with Rometar (10 mg/kg) and immobilized in a side position, the center of the tumor was placed into the center of the scanning area.

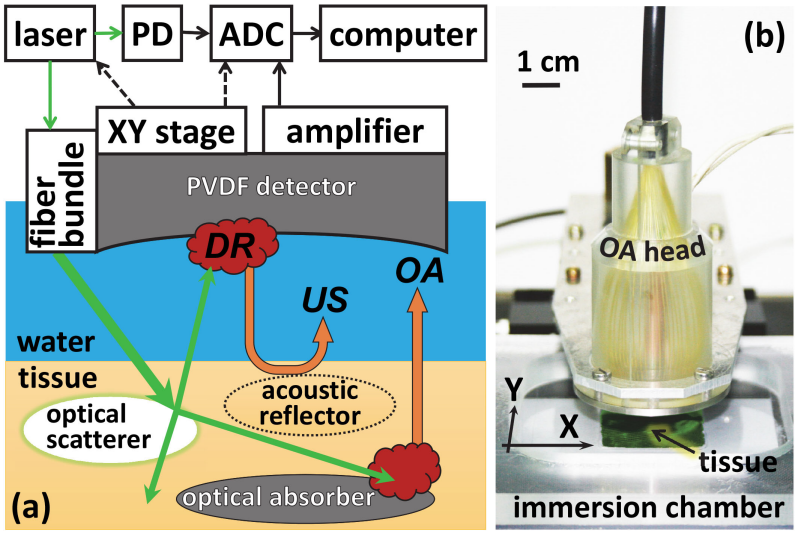

Fig. 1. The schematic (a) and picure (b) of the experimental setup for simultaneous DR/OA/US/ imaging.

Biomedical Optics EXPRESS

All *in vivo* objects were scanned in xy-plane with 25 μm step size. Each laser pulse triggered a 16 bit two-channel CSE1622 (Gage, USA) analog-to-digital converter (ADC) to collect the beam-sampling signal from a det10a (Thorlabs, USA) photodiode (PD) and DR/OA/US A-scans from PVDF detector. PD contained a custom-made built-in integration circuit expanding the effective pulse duration to ~50 ns for better compatibility with the 200 MS/s acquisition rate of the ADC. The PVDF detector had a custom-made 30 dB amplifier with a 3 MHz high-pass filter. An acquisition algorithm recorded the time-spaced DR/OA/US signals to corresponding B-scans. Temporal shapes of PD signals were used to eliminate jitter effect of the laser. Amplitudes of PD signals were used to normalize OA and DR signals. Since each DR signal is probing US pulse, US signals were then normalized by amplitudes of DR signals. After complete set of 3D data was acquired, OA and US signals were processed using virtual-detector concept [16] and acoustic inversion algorithm [17]. Finally, the maximum intensity projections (MIP) of DR/OA/US A-scans were calculated to form corresponding DR/OA/US images of the investigated objects.

3. Results and discussion

The pecularities of vascular development within various tumor models are often used to demonstrate *in vivo* performance of the novel OA imaging systems [18, 19]. Figure 2 represents the results of simultaneous DR/OA/US imaging of SKBR3 tumor model. Superficial blood vessels seen at the photograph of the tumor (Fig. 2(a)) are marked by yellow arrows.

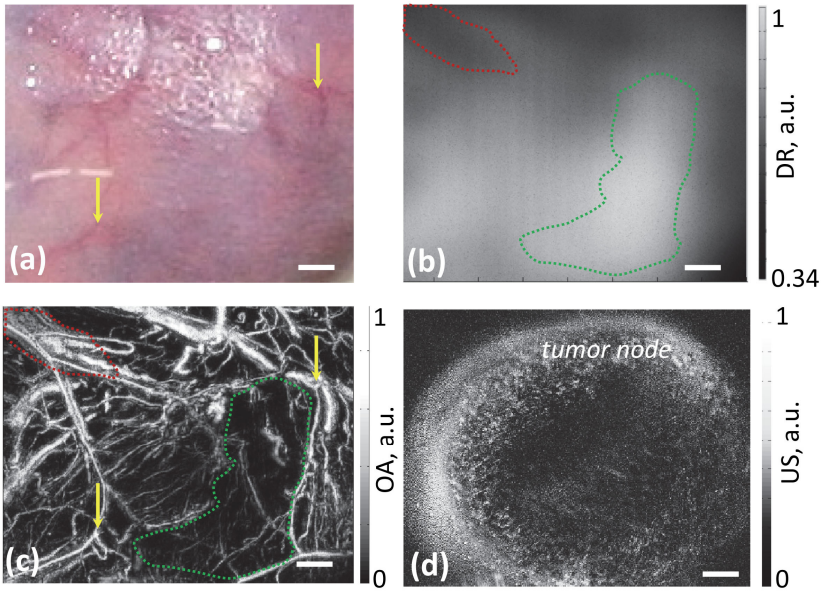

Fig. 2. The results of simultaneous DR/OA/US imaging of the SKBR3 tumor, all bars are 1 mm. (a) – photograph of tumor in vivo, (b) – MIP DR image; (c) – MIP OA image; (d) – MIP US image. Yellow arrows indicate superficial blood vessels, red and green dots indicate the regions with high and low hemoglobin content corespondingly.

DR image (Fig. 2(b)) indicates non-homogeneous spatial distribution of absorbing and scattering structures within the tumor volume. Zones with low DR signal can be presented by haemorrhages or by areas with high vessels density. OA image (Fig. 2(c)) demonstrates the spatial distribution of individual blood vessels located at different depths of the tumor (with superficial vessels marked by yellow arrows) and characterizes the same zones as the regions with high vessels density. OA modality also characterizes high vascularization of the SKBR3

Biomedical Optics EXPRESS

tumor with large amount of small randomly distributed blood vessels. At DR and OA images (Fig. 2(b), 2(c)) the regions with high blood content are marked by red dots, while the regions with low blood content are marked by green dots.

US image (Fig. 2(d)) represents the contours of the tumor node. Structural information provided by US image complements functional information provided by DR and OA images and allows to differentiate blood supply of normal and tumor tussues.

Experimental validation of the new OA methods is often performed by means of mouse brain imaging *in vivo* [20, 21]. Figure 3 represents the results of simultaneous DR/OA/US imaging of rat's head. Two small haemorrhages at the surface of the rat skin are well seen at the photograph image (Fig. 3(a)) and are marked by yellow arrows. DR image indicates the dark zones being the projections of transverse and saggital sinuses. The position of confluence of sinus is marked by red-dotted region at Fig. 3(b). The transverse and saggital sinuses with the their confluence are also seen at OA image (Fig. 3(c)). However, due to the deeper location of sinuses under the skull bones, superficial blood vessels appear at OA image with higher contrast. The highest OA contrast is demonstrated by haemorrhages located at the surface of rat's skin. Using US image (Fig. 3(d)) it is possible to define different skull bones and confirm the relative positions of blood vessels and sinuses.

Figure 4 presents the results of simultaneous DR/OA/US imaging of chest region of the rat's back. OA image demonstrates the positions of larger blood vessels located along the vertebral column as well as smaller superficial vessels. US image allows to determine the positions of vessels in relation to vertebra and ribs. Low quality of DR image can be explained by the breathing activity of laboratory animal. The position of optical focus changed during the experiment and appeared as vertical lines at DR image.

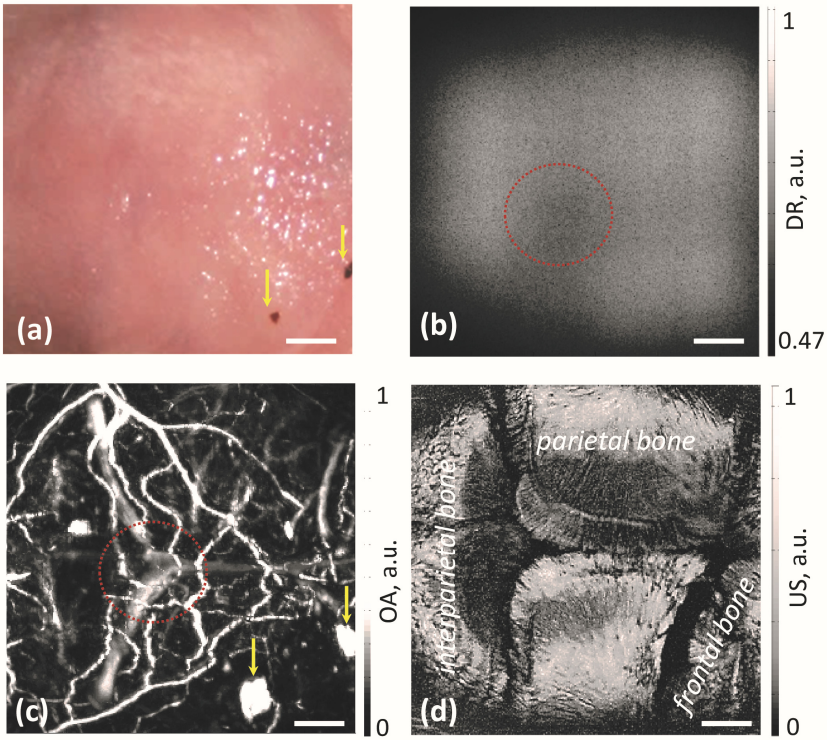

Fig. 3. The results of DR/OA/US imaging of the rat's head, all bars are 1 mm. (a) – photograph of the rat's head in vivo, (b) – MIP DR image; (c) – MIP OA image; (d) – MIP US image. Yellow arrows indicate haemorrhages located at the skin's surface; red dots indicate the region with high hemoglobin content.

Biomedical Optics EXPRESS

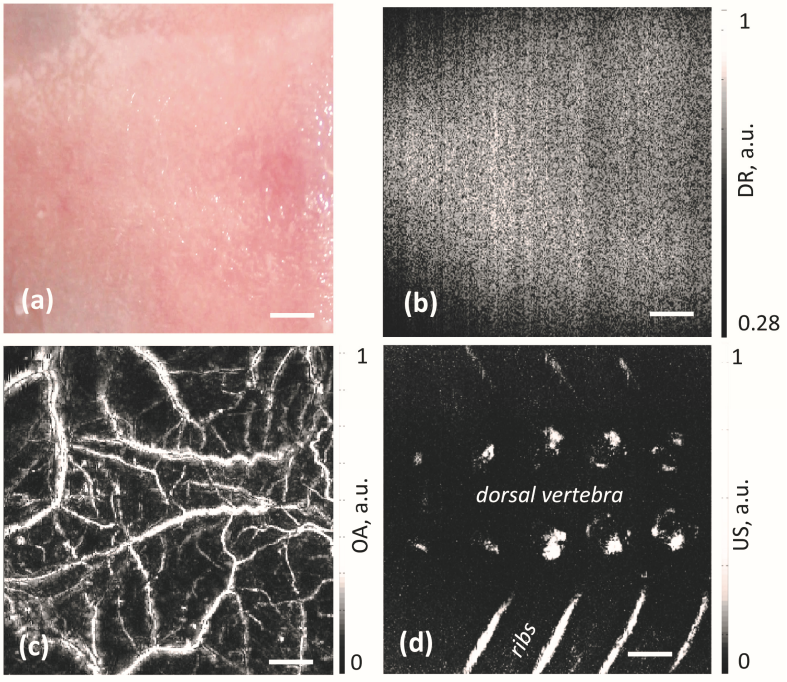

Fig. 4. The results of DR/OA/US imaging of the rat's back, all bars are 1 mm. (a) – photograph of the rat's back, (b) – MIP DR image; (c) – MIP OA image; (d) – MIP US image.

According to the results of phantom experiments [14], the regions with high DR signal (Figs. 2-3) can characterize not only low local optical absorbtion, but also high local optical scattering. Therefore, some features of *in vivo* DR images can also be connected with inhomogeneous distribution of optical scatterers. Non-homogeneous distribution of optical scattering coefficient can result in the non-uniform contrast at MIP OA image, since the spatial distribution of optical scatterers is non-locally connected with the optical fluence, determining the intensity of OA pulse (Fig. 1).

The ability of DR and OA modalities to sence both scattering and absorbing heterogeneities allows to simplify quantitative optoacoustic imaging [22]. However, to separate sattering and absorbing properties using DR and OA measurements, one requires proper mathematical model [23]. The process of DR/OA measurements from non-homogeneous tissue by fixed geometry of the light delivery and the detection (Fig. 1) can be simulated using Monte-Carlo modeling of light transport [24]. US measurements can allow complementary determination of the investigated tissue geometry for Monte-Carlo model.

The transition from single-wavelength to multispectral measurements is possible technological improvement of the proposed trimodal system. Additional probing optical wavelengths may allow to determine the oxygen saturation in regions imaged by DR/OA/US modalities, or even provide quantitative measurements of other tissue chromophore concentrations with known optical spectra [25].

4. Conclusion

Therefore, this article presents the results of *in vivo* approbation of trimodal experimental setup based on acoustic resolution photoacoustic microscope. To realize complementary DR and US measurements, our system utilizes the photons emerging from optical scatterers within the investigated object towards an acoustic detector. The absorbtion of back-scattered

Biomedical Optics EXPRESS

photons on detector's surface causes the measurable DR signal and probing US pulse at the same time.

Functional OA and DR imaging demonstrated the level of tissue vascularization and blood supply. Structural US imaging was essential for understanding the position of vessels and zones with different perfusion.

Fourfold improvement in lateral resolution of OA/US modalities resulted in more detailed *in vivo* images of all three localizations, as compared to the performance of previously-reported dual-modality OA/US system [12]. *In vivo* performance of DR modality is demonstrated by DR images of two localizations (tumor and head). Due to the breathing activity of the animal, DR image of rat's back did not allow locating the regions with non-homogeneous distribution of optical parameters.

Along with the imaging of the optical and acoustic heterogeneities, we propose to use the developed method of trimodal DR/OA/US registration for quantitative measurements. However, to reconstruct tissue chromophore concentrations it is important to provide multispectral DR/OA/US measurements and use proper Monte-Carlo simulation for non-homogeneous tissues and the geometries of the light delivery and detection.

Funding

Russian Science Foundation (project #14-15-00709), Dr. Pavel Subochev was partly supported by Scholarship of the President of the Russian Federation (project #SP-3196.2016.4).

Acknowledgment

The authors are grateful to Maxim Prudnikov, Roman Belyaev and Vladimir Vorobyev for their engineering contributions to this work and to Dr. Michael Jaeger for provision of reconstruction algorithm.

194.190.189.26 {ts '2016-09-13 04:28:04'}